Increasing the interlayer distance in layered microribbons enhances the electrically driven twisting response

Yifan Zhang,[1,2,3] Zichao Zhou,[1,2] Cheng Peng,[1,2] Ran Duan,[1] Yanke Che,[1,2,*] and Jincai Zhao[1,2]

[1]*Key Laboratory of Photochemistry, Institute of Chemistry, Chinese Academy of Sciences, Beijing 100080, China*
[2]*University of Chinese Academy of Sciences, Beijing 100049, China*
[3]*IBS Center for Soft and Living Matter, Ulsan National Institute of Science and Technology, Ulju-gun, Ulsan 689-789, South Korea*

We designed a class of layered microribbons self-assembled from perylene diimide (PDI) molecules that exhibited a fast electrically driven twisting response. By increasing the length of the side chains of the PDIs, the microribbons maintained the same intralayer molecular orientation but exhibited enlarged interlayer distances, and the elasticity moduli of the resulting layered microribbons were effectively reduced from ∼1.5 GPa to ∼75 MPa. The electrically driven twisting response of the microribbons was inversely proportional to the elasticity modulus, indicating that the electroresponse of the resulting materials can be controlled through the interlayer distance. Furthermore, we demonstrated that the influence of the elastic modulus of the microribbons on the electrically driven twisting follows a screw dislocation mechanism. Our work provides a way to design and develop soft materials with a fast mechanical response to external stimuli.

Soft materials that change morphology in response to external stimuli, particularly remote light or electrons, have attracted considerable interest because of their applications in actuators and sensors [1–24]. In these applications, a fast mechanical response, which is related to both the active components (e.g., photoisomers) and the elasticity of the soft material, is one of the most important parameters [15,25,26]. Although various soft materials with fast mechanical responses have been reported, most seemed to have been developed based on serendipitous discovery or random screening and no general design principles have been reported. This is likely because subtly modifying the structure of the active components simultaneously alters intermolecular interactions and crystal structures, which in turn change the elasticity of the resulting materials. This complicated situation has hampered the creation of a rational molecular design for soft materials with a fast mechanical response. The rational development of response-controlled soft materials is critical to not only the comprehensive understanding of fast mechanical responses but also the development of novel response-sensitive materials, but the highly desirable development of addressable methods remains rare. One promising strategy is fabricating layered materials whose elasticity modulus can be adjusted by tuning the interlayer distance while maintaining the intralayer molecular organization of the active monomers [27,28] and thereby the same driving force in response to stimuli.

In this work, we designed a class of layered microribbons self-assembled from perylene diimide (PDI) molecules, which exhibited a fast electrically driven twisting response. We demonstrated that the elasticity moduli of the resulting layered microribbons were effectively reduced from ∼1.5 GPa to ∼75 MPa by increasing the length of the alkyl side chains. Importantly, the increased alkyl side chain length did not alter the intralayer molecular orientation but enlarged the interlayer distance of the microribbon, which is related to the reduced elasticity modulus. The electrically driven twisting response of the microribbons was inversely proportional to the elasticity modulus, indicating that the electro-response of the resulting materials can be controlled by the interlayer distance. Furthermore, we demonstrated that a screw dislocation mechanism underlies the electrically driven twisting of the layered microribbons, revealing how the electrically driven π-stacking distortion generates the twisting of the microribbon.

Nine PDI derivatives with different lengths of alkyl side chains were synthesized [as shown in Fig. 1(a)] and self-assembled into microribbons. The synthesis and self-assembly of the molecules are presented in detail in the Supplemental Material [29]. Scanning electron microscopy (SEM) confirmed the formation of well-defined microribbons from molecules **1**–**9**, which are tens of micrometers in length and 0.3–0.8 μm in width [Figs. 1(b)–1(e) and Fig. S1]. Notably, the resulting microribbons fabricated from molecules **1**–**9** have fairly similar optical properties, as shown in Fig. 2(a). All microribbons from molecules **1**–**9** exhibited characteristic absorptions at 490, 527, and 575 nm and fluorescence at 629 nm, suggesting that they have similar molecular orientations and thus the same excitonic coupling within the microribbon. To further explore the molecular packing within microribbons, we performed x-ray diffraction (XRD) on the microribbons from molecules **1**–**9**. As shown in Figs. 2 and S2, a dominant peak assignable to the (001) plane was observed in the XRD patterns of all microribbons, which is characteristic of a lamellar (layered) structure [30,31]. The multiple sharp reflections indicate that the layered microribbons are highly crystalline. The XRD patterns of the microribbons from **1**, **4**, and **9** are consistent with their single crystal data [Figs. 2(b)–2(d)], indicating that the lattice parameters within the microribbons are the same as those in the bulk crystal [32,33]. To determine the lattice parameters within the microribbons from molecules **2**–**3** and **5**–**8**, selected-area electron diffraction (SAED) patterns of the corresponding microribbons were obtained, which can help determine the d-spacing values of the (100) and (010) planes and the γ value, as shown in Fig. S3. Based on the
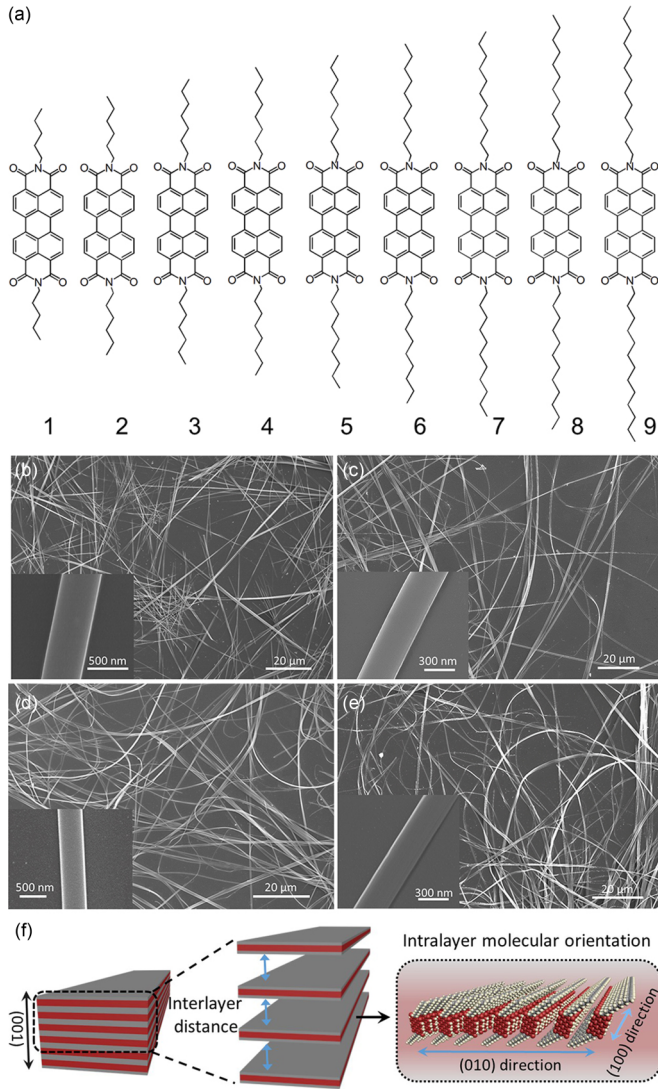
*ykche@iccas.ac.cn

FIG. 1. (a) Molecular structures of molecules **1–9**. (b)–(e) SEM images of the microribbons from **1** (b), **5** (c), **7** (d), and **9** (e). Insets: a high-magnification image of a single corresponding microribbon. (f) Schematic representation of the molecular packing within a layered microribbon.

FIG. 2. (a) UV-vis and fluorescence spectra of the microribbons from **1** to **9**. (b)–(d) Experimental and calculated XRD patterns of the microribbons from **1** (b), **4** (c), and **9** (d). (e) The molecular arrangement within the microribbons from **1**, **4**, and **9**.

SAED and XRD patterns, the molecular packing within the microribbons from 2–3 and 5–8 was simulated (Fig. S4). The lattice parameters of the microribbons from 1–9 are summarized in Table I. Clearly, the molecular orientation along the (100) and (010) directions within the microribbons from **1–9** [as indicated in Fig. 1(f)] are similar (Table I), while the interlayer distance along the (001) direction increases with the length of the side chain (Table I). Notably, a dramatic change in the interlayer distance along the (001) direction (i.e., from 1.6 to 2.6 nm) has no effect on the optical properties of the resulting microribbons [Fig. 2(a)]. This observation indicates that the interlayer molecular packing is excitonic uncoupling, while the intralayer molecular packing exhibits a strong excitonic coupling and determines the optical properties. This result is reminiscent of other weakly coupled excitonic bilayer systems separated by long alkyl chains [34].
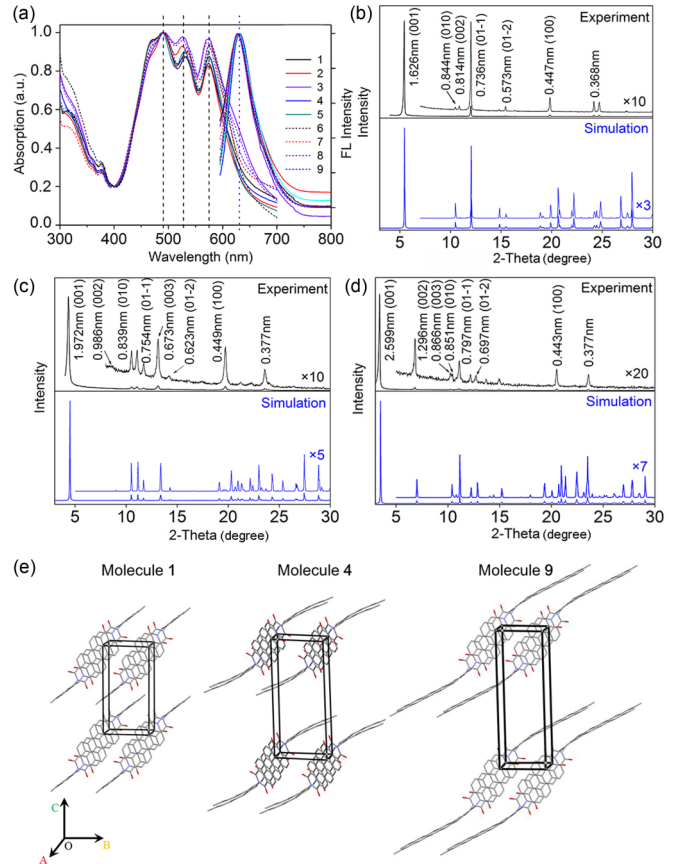
We observed that the microribbons with longer alkyl side chains became angled and curved with the increasing interlayer distance (as shown in Figs. 1 and 2, as well as Fig. S4), suggesting that the microribbons softened with larger interlayer distances. To corroborate this, we used atomic force microscopy (AFM) to perform a three-point bending test [35] on microribbons bridged over a trench on a Si wafer, which allowed precisely measuring the elastic modulus [Fig. 3(a)]. The surface of the microribbon is smooth (Fig. S5), thereby excluding the possible influence of large defects on the elastic modulus. By following the reported method, the

TABLE I. Lattice parameters of the microribbons from **1** to **9**.

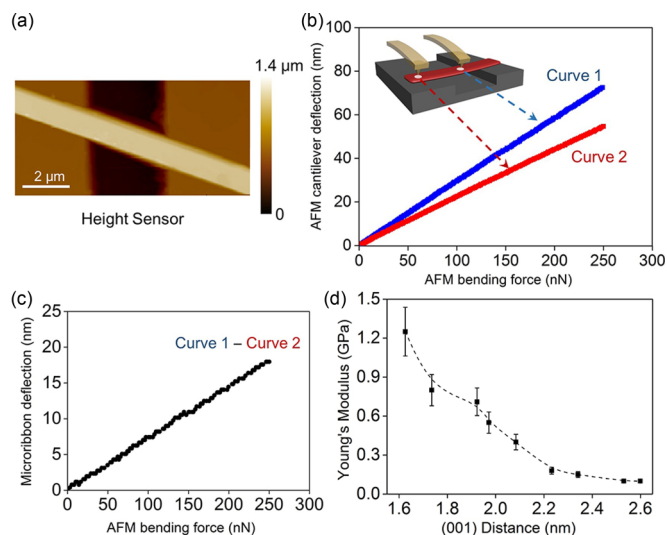| Molecule	a (Å)	b (Å)	c (Å)	α	β	γ
1	4.47	8.44	16.26	87°	84°	85°
2	4.48	8.40	17.34	87°	88°	89°
3	4.41	8.38	19.23	87°	86°	88°
4	4.49	8.39	19.72	86°	88°	83°
5	4.49	8.48	20.84	87°	86°	89°
6	4.40	8.50	22.31	85°	86°	82°
7	4.38	8.39	23.41	86°	86°	82°
8	4.37	8.52	24.96	86°	86°	82°
9	4.43	8.51	25.99	86°	86°	82°

FIG. 3. (a) Height-mode AFM image of a typical microribbon assembled from **1** that bridged a trench on a Si substrate. (b) AFM bending force as a function of the AFM cantilever deflection (curve 1) and the baseline curve measured at a site where the microribbon was located on the silica (curve 2). (c) Applied bending force as a function of the microribbon deflection. (d) Elastic modulus as a function of the interlayer distance of the microribbons from **1** to **9**.

AFM cantilever deflection−AFM bending force curve (curve 1) was obtained from a typical bridged microribbon assembled from 1 [Fig. 3(b)]. This curve represents the total AFM tip deflection and exhibits both the effect of indentation by the tip on the microribbon and the microribbon deflection. To eliminate the indentation effect, a baseline curve (curve 2) was also measured on a site of the microribbon located on the silica. Subtracting curve 2 from curve 1 yielded the bending force−microribbon deflection relationship of the microribbon from molecule **1**, as shown in Fig. 3(c). The corresponding data from the other microribbons were obtained in the same way. Based on these results, the spring constant, K_n, of each microribbon was calculated from the reciprocal of the slope of the linear curve of the applied microribbon deflection−AFM bending force. Assuming that the microribbons comply with the linear elastic theory, the elastic modulus of a microribbon, E_n, can be calculated from the following equation:

$$E_n = \frac{k_n L^3}{192 I},$$

where I is the moment of inertia. For a rectangular microribbon (Fig. S6), $I = wh^3/12$, where w and h are the width and height of the microribbon, respectively. L is the suspended length of the microribbon, and K_n is the spring constant of the microribbon. The dimensional parameters and Young's modulus of each microribbon from **1** to **9** are summarized in Table S1. Figure 3(d) shows the calculated elastic moduli of the microribbons assembled from **1** to **9** (at least three microribbons were tested per structure). The elastic moduli dramatically decreased with the increasing microribbon interlayer distance from 1.3 ± 0.15 GPa (microribbon **1**) to 100 ± 15 MPa (microribbon **9**). These observations indicate that longer alkyl side chains enable larger interlayer distances
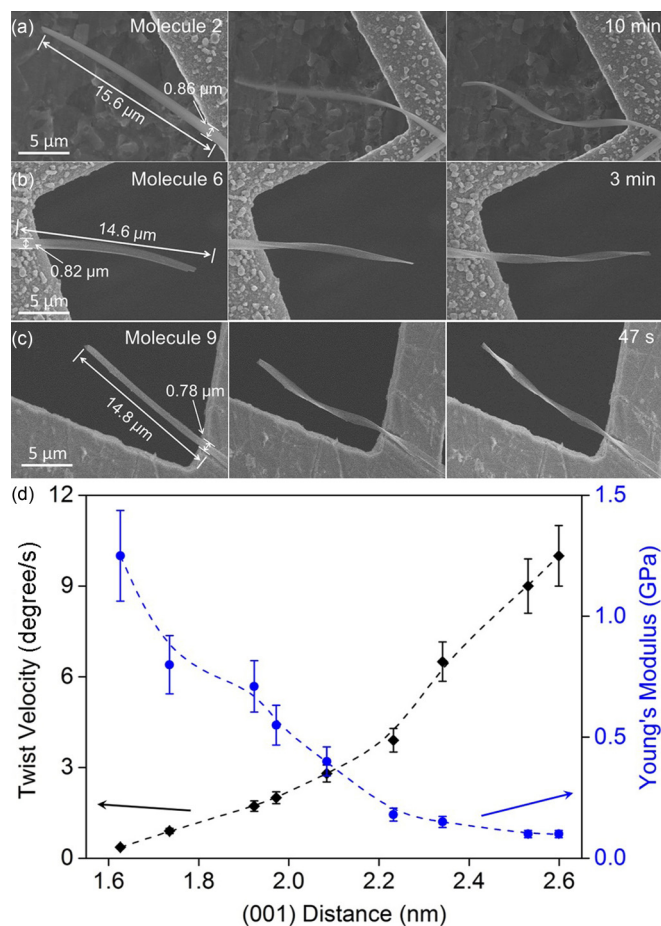

FIG. 4. The time-dependent morphological changes of typical microribbons from **2** (a), **6** (b), and **9** (c) when exposed to a scanning electron beam during SEM measurements (10 KV, 10 μA, 600 K). (d) Twist velocity (black line) and elastic modulus (blue line) as a function of the interlayer distance of the microribbons from **1** to **9**. At least six microribbons with similar crystal size were examined for each type of microribbon.

and in turn decrease the elastic modulus of the resulting material.

We previously reported that electrons are capable of inducing a π-stacking distortion through the temporary occupation of the lowest unoccupied molecular orbital of a PDI monomer within a microribbon and thus give rise to a PDI anionic radical; this was found to further translate into macroscopic morphological changes [18]. Inspired by these results, we postulated that the electrically driven π-stacking distortion would remain similar within the microribbons from **1** to **9** because of the similar intralayer molecular packing of the perylene cores; a reduced elastic modulus is expected to enhance the microribbons' response to electrons. To validate our hypothesis, we cast the assembled microribbons onto a copper grid and selected those with one end free to explore the electrically driven morphological changes (Fig. 4). All microribbons from **1** to **9** underwent twisting upon exposure to the electron beam from SEM measurements (Figs. 4(a)–4(c) and Fig. S7). Typically, a microribbon (∼15 μm in length and ∼0.8 μm in width) from molecule **2** took ∼10 min to

TABLE II. Dimensional parameters of eight microribbons from **2**.

No.	L_{twist} (μm)	W (μm)	T (μm)	S (μm^2)
1	9.08 ± 0.05	0.72 ± 0.01	0.21 ± 0.02	0.1512 ± 0.0165
2	8.12 ± 0.05	0.71 ± 0.01	0.20 ± 0.01	0.1420 ± 0.0091
3	11.40 ± 0.07	0.88 ± 0.01	0.19 ± 0.02	0.1672 ± 0.0195
4	6.04 ± 0.05	0.41 ± 0.01	0.16 ± 0.02	0.0656 ± 0.0098
5	5.74 ± 0.04	0.69 ± 0.01	0.12 ± 0.01	0.0828 ± 0.0081
6	9.80 ± 0.06	0.51 ± 0.01	0.25 ± 0.02	0.1275 ± 0.0127
7	8.94 ± 0.04	0.48 ± 0.01	0.17 ± 0.02	0.0816 ± 0.0113
8	19.14 ± 0.08	0.98 ± 0.01	0.31 ± 0.02	0.3038 ± 0.0227

twist a full 540° [Fig. 4(a)], while microribbons from **6** and **9** with similar dimensions took only 3 min [Fig. 4(b)] and 47 s [Fig. 4(c)], respectively, to finish the same twisting process. The dependence of twisting velocity with the increasing of interlayer distance is concluded in Fig. 4(d). Note that the twisting of the microribbons was not reversible, likely because an irreversible molecular reorganization within the microribbons occurred during the morphological change. These results clearly confirm that the electrically driven twisting response of the microribbons can be effectively controlled by the elastic modulus, which is successfully tuned by the interlayer distance within the layered microribbons.

To further reveal how the electrically driven π-stacking distortion generates the twisting of the microribbon, we used the screw-dislocation model [36–38] and interfacial strain model [19] to analyze the periodic twisting behaviors. Here, we chose microribbons assembled from **2** because they exhibit a proper twisting rate and an appropriate stiffness to easily deposit them with one end free on a copper grid. The dimensions of eight microribbons assembled from **2** [including width (W), thickness (T) and pitch length (L_{twist})] were measured, and the results are summarized in Table II. Given that the microribbon has a rectangular cross section, as confirmed by the AFM image, the area of the cross section of the microribbon (S) was calculated from W and T (Table II). By fitting our data to the screw-dislocation theory,

$$L_{twist} = \frac{2\pi k S}{b}, \tag{1}$$

where k is a constant on the order of unity, and b is the magnitude of the screw-dislocation defect dependent on the Burgers vector. A line with a slope of 69.537 and a good R^2 value of 0.96 were obtained (Fig. 5). Thus, a value of $b = 0.09\,\mu$m was obtained (k was set as 1) to predict the void diameter (D) of the twisted microribbon using the following equation:

$$D = \frac{Gb^2}{4\pi^2\gamma} = \frac{Eb^2}{8(1+\mu)\pi^2\gamma}, \tag{2}$$

where E is the elastic modulus, μ is Poisson's ratio, and γ is the surface energy. When we set Poisson's ratio as $\mu = 0.3$ [39] and $\gamma = 0.2\,$J/m^2 [40] (typical values for organic materials), a value of $D = 0.32\,\mu$m was obtained for the microribbon from **2** with an elastic modulus of 800 MPa. This calculated D value agrees well with the experimental value of $D = 0.43\,\mu$m, as shown in Fig. 4(a). The above linear fit and the consistency
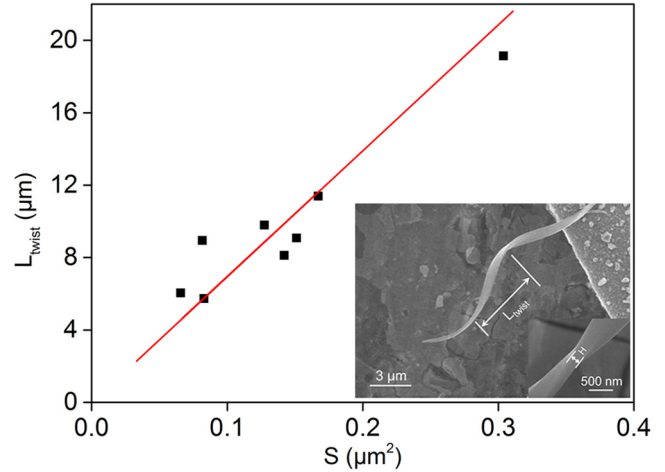

FIG. 5. Linear fit of the pitch length of the twisted microribbons as a function of the cross-sectional area with Eq. (1), resulting in a slope of 69.537 and an R^2 of 0.96 (R^2 represents the coefficient of determination of the linear fit).

of the calculated and experimental D values indicate that the twisting of the microribbon follows the screw-dislocation mechanism, i.e., the diagonal force relative to the microribbon axis generated from electrical excitation induced the screw dislocation of the monomers within the microribbon and in turn the macroscopic twisting of the whole microribbon.

We also fit our data to the interfacial strain model [19] and obtained a linear fit with a poor quality of $R^2 = 0.87$ (Fig. S8), indicating that the interfacial strain mechanism, which usually operates in systems containing a photochemical reaction or photoisomers [9,19,20,41,42], is not operative in our twisted microribbons. Here, a notable feature of our system is the application of π-stacking distortion rather than widely used molecular motors or switches as the electroactive components, which would conveniently enrich electroresponsive systems based on a wide range of organic crystals.

In conclusion, we report a class of layered microribbons self-assembled from PDI molecules, which exhibited fast electrically driven twisting. We demonstrated that the elasticity moduli of the resulting layered microribbons can be effectively reduced (i.e., from 1.5 GPa to 75 MPa) by only increasing the interlayer distance (by increasing the length of the alkyl side chains) without interrupting the intralayer molecular orientation. The reduced elasticity modulus favors the electrically driven twisting, resulting in an inverse dependence of the twisting rate on the elasticity modulus. Analyzing the mechanism indicated that the twisting of the microribbons arises from a screw dislocation of the monomers by a diagonal π-stacking distortion relative to the microribbon axis, which in turn translates into the macroscopic twisting of the whole microribbon. This work presents a way of developing soft materials with a fast response to external stimuli. We expect that controlling the interlayer spacing by designing functional side chains of various lengths could be extended to modulating the mechanical properties of other layered materials under different circumstances, such as graphene [43], graphene oxide nanomaterials [27], perovskites [44–47], and other soft materials [28,48–51].

[1] W. R. Browne and B. L. Feringa, Nat. Nanotechnol. **1**, 25 (2006).

[2] S. Kobatake, S. Takami, H. Muto, T. Ishikawa, and M. Irie, Nature (London) **446**, 778 (2007).

[3] M. A. Garcia-Garibay, Angew. Chem., Int. Ed. **46**, 8945 (2007).

[4] Y. Nabetani, H. Takamura, Y. Hayasaka, T. Shimada, S. Takagi, H. Tachibana, D. Masui, Z. Tong, and H. Inoue, J. Am. Chem. Soc. **133**, 17130 (2011).

[5] M. Morimoto and M. Irie, J. Am. Chem. Soc. **132**, 14172 (2010).

[6] Y. Liu *et al.*, J. Am. Chem. Soc. **127**, 9745 (2005).

[7] F. Terao, M. Morimoto, and M. Irie, Angew. Chem., Int. Ed. **51**, 901 (2012).

[8] J. Berna, D. A. Leigh, M. Lubomska, S. M. Mendoza, E. M. Perez, P. Rudolf, G. Teobaldi, and F. Zerbetto, Nat. Mater. **4**, 704 (2005).

[9] T. Ikeda, J.-i. Mamiya, and Y. Yu, Angew. Chem., Int. Ed. **46**, 506 (2007).

[10] H. Koshima, N. Ojima, and H. Uchimoto, J. Am. Chem. Soc. **131**, 6890 (2009).

[11] S. Iamsaard, S. J. Asshoff, B. Matt, T. Kudernac, J. J. L. M. Cornelissen, S. P. Fletcher, and N. Katsonis, Nat. Chem. **6**, 229 (2014).

[12] N. Hosono, T. Kajitani, T. Fukushima, K. Ito, S. Sasaki, M. Takata, and T. Aida, Science **330**, 808 (2010).

[13] M. Yamada, M. Kondo, J.-i. Mamiya, Y. Yu, M. Kinoshita, C. J. Barrett, and T. Ikeda, Angew. Chem., Int. Ed. **47**, 4986 (2008).

[14] C. L. van Oosten, C. W. M. Bastiaansen, and D. J. Broer, Nat. Mater. **8**, 677 (2009).

[15] T. J. White and D. J. Broer, Nat. Mater. **14**, 1087 (2015).

[16] H. Finkelmann, E. Nishikawa, G. G. Pereira, and M. Warner, Phys. Rev. Lett. **87**, 015501 (2001).

[17] T. Kudernac, N. Ruangsupapichat, M. Parschau, B. Macia, N. Katsonis, S. R. Harutyunyan, K.-H. Ernst, and B. L. Feringa, Nature (London) **479**, 208 (2011).

[18] Y. Zhang, C. Peng, Z. Zhou, R. Duan, H. Ji, Y. Che, and J. Zhao, Adv. Mater. **27**, 320 (2015).

[19] L. Zhu, R. O. Al-Kaysi, and C. J. Bardeen, J. Am. Chem. Soc. **133**, 12569 (2011).

[20] T. Kim, L. Zhu, L. J. Mueller, and C. J. Bardeen, J. Am. Chem. Soc. **136**, 6617 (2014).

[21] H.-J. Kim, T. Kim, and M. Lee, Acc. Chem. Res. **44**, 72 (2011).

[22] E. Ohta *et al.*, Nat. Chem. **3**, 68 (2010).

[23] P. V. Kamat, T. K. George, B. Said, G. Girishkumar, K. Vinodgopal, and M. Dan, J. Am. Chem. Soc. **126**, 10757 (2004).

[24] M. Irie, S. Kobatake, and M. Horichi, Science **291**, 1769 (2001).

[25] N. Koumura, E. M. Geertsema, M. B. van Gelder, A. Meetsma, and B. L. Feringa, J. Am. Chem. Soc. **124**, 5037 (2002).

[26] D. Pijper, R. A. van Delden, A. Meetsma, and B. L. Feringa, J. Am. Chem. Soc. **127**, 17612 (2005).

[27] C. Cao, M. Daly, B. Chen, J. Y. Howe, C. V. Singh, T. Filleter, and Y. Sun, Nano Lett. **15**, 6528 (2015).

[28] N. Seiki, Y. Shoji, T. Kajitani, F. Ishiwari, A. Kosaka, T. Hikima, M. Takata, T. Someya, and T. Fukushima, Science **348**, 1122 (2015).

[29] See Supplemental Material at http://link.aps.org/supplemental/10.1103/PhysRevMaterials.1.033601 for the details of the synthesis and self-assembly of the molecules from 1 to 9.

[30] Y. Che, X. Yang, G. Liu, C. Yu, H. Ji, J. Zuo, J. Zhao, and L. Zang, J. Am. Chem. Soc. **132**, 5743 (2010).

[31] S. Yagai *et al.*, J. Am. Chem. Soc. **134**, 7983 (2012).

[32] E. H. Hadicke and F. Graser, Acta Crystallogr., Sect. C: Struct. Chem. **42**, 189 (1986).

[33] S. Tatemichi, M. Ichikawa, T. Koyama, and Y. Taniguchi, Appl. Phys. Lett. **89**, 112108 (2006).

[34] D. M. Eisele *et al.*, Nat. Chem. **4**, 655 (2012).

[35] Y. Yingchao, W. Guofeng, and L. Xiaodong, Nano Lett. **11**, 2845 (2011).

[36] K. Kawabata, T. Kumagai, M. Mizutani, and T. Sambongi, J. Phys. I (France) **6**, 1575 (1996).

[37] A. L. McClellan, J. Chem. Phys. **32**, 1271 (1960).

[38] J. D. Eshelby, J. Appl. Phys. **24**, 176 (1953).

[39] K. Nakamae, T. Nishino, and A. Xu, Polymer **33**, 4898 (1992).

[40] D. Nabok, P. Puschnig, and C. Ambrosch-Draxl, Phys. Rev. B **77**, 245316 (2008).

[41] P. D. Calvert and D. R. Uhlmann, J. Polym. Sci.: Polymer Physics Edition **11**, 457 (1973).

[42] A. G. Shtukenberg, J. Freudenthal, and B. Kahr, J. Am. Chem. Soc. **132**, 9341 (2010).

[43] E. Yoo, J. Kim, E. Hosono, H.-s. Zhou, T. Kudo, and I. Honma, Nano Lett. **8**, 2277 (2008).

[44] B. Saparov and D. B. Mitzi, Chem. Rev. **116**, 4558 (2016).

[45] S. Kataoka, S. Banerjee, A. Kawai, Y. Kamimura, J.-C. Choi, T. Kodaira, K. Sato, and A. Endo, J. Am. Chem. Soc. **137**, 4158 (2015).

[46] D. Umeyama, Y. Lin, and H. I. Karunadasa, Chem. Mater. **28**, 3241 (2016).

[47] A. K. Geim and I. V. Grigorieva, Nature (London) **499**, 419 (2013).

[48] W. Zhang, W. Jin, T. Fukushima, N. Ishii, and T. Aida, Angew. Chem., Int. Ed. **48**, 4747 (2009).

[49] C. Peng, Y. Zhang, Y. Zhang, Y. Hu, Y. Che, and J. Zhao, Small **12**, 4363 (2016).

[50] K. Balakrishnan, A. Datar, R. Oitker, H. Chen, J. Zuo, and L. Zang, J. Am. Chem. Soc. **127**, 10496 (2005).

[51] H. Langhals, Heterocycles **40**, 477 (1995).